Title

Unraveling the Core: Hub Genes Bridging Familial and Sporadic Parkinson's Disease

Author names

Simran Singh[a], Gulshan Chauhan[a], Baisakhi Moharana[b], Sonia Verma[a*]

Affiliations

[a]Division of Neuroscience and Ageing Biology, CSIR-Central Drug Research Institute, Lucknow, UP, India; Academy of Scientific and Innovative Research (AcSIR), Ghaziabad 201002, India.

[b]Division of Pharmacology, CSIR-Central Drug Research Institute, Lucknow, UP, India; Academy of Scientific and Innovative Research (AcSIR), Ghaziabad 201002, India.

[*]Corresponding Author

Sonia Verma, Scientist, Division of Neuroscience and Ageing Biology, CSIR-Central Drug Research Institute, Lucknow, UP, India. E-mail address: sonia.verma1@gmail.com (Verma S.).

Abstract

Parkinson's disease (PD), a neurodegenerative disorder characterized by dopaminergic (DA) neuron loss in the substantia nigra, manifests as familial (genetically linked) or idiopathic (sporadic) forms. Despite distinct etiologies, both subtypes converge on shared pathological mechanisms that remain poorly understood. This study focused on identifying "hub genes" that might drive DA neuron degeneration in familial and idiopathic PD. The gene expression data from three publicly available datasets were reanalyzed. These datasets included samples from DA neurons derived from postmortem brains and patient-derived induced pluripotent stem cells. Twelve hub genes were identified to be dysregulated across all three datasets. The hub genes were found to play vital roles in membrane trafficking and vesicle-mediated transport. NetworkAnalyst-based reconstruction linked these hub genes to various other diseases. Experimental validation in neurotoxin-induced SH-SY5Y cell models of PD confirmed significant changes in the mRNA levels of some of the hub genes. Crucially, silencing one of the hub genes in *Caenorhabditis elegans* promoted DA neuron degeneration. Our study identifies potential candidates as therapeutic targets for DA neuron degeneration in familial and idiopathic PD.

Keywords

Dopaminergic Neurons; Familial Parkinson's disease; Idiopathic Parkinson's disease; Hub genes; Neurodegeneration; Novel Therapeutic Targets

1. Introduction

Parkinson's disease (PD) is a multifaceted neurodegenerative disorder predominantly characterized by the progressive degeneration of dopaminergic (DA) neurons in the substantia nigra pars compacta, leading to hallmark motor deficits and non-motor symptoms [1,2]. PD is broadly classified into two categories based on etiology: familial PD and idiopathic PD. Familial PD accounts for 5-10% of all cases and has been linked to mutations in pivotal genes such as *SNCA*, *LRRK2*, *PARK2*, *PINK1*, *DJ-1*, and *GBA*, each contributing to distinct cellular dysfunctions, including mitochondrial stress, impaired autophagy, proteostasis disruption, and lysosomal dysfunction [3-18]. Genome-wide association studies (GWAS) have further identified novel risk loci such as *TMEM175*, *GAK*, and *BST1*, extending the genetic landscape of PD pathogenesis [19,20]. Idiopathic PD accounts for approximately 90-95% of all PD cases [21]. There are no clear genetic links in idiopathic cases, and individuals affected by this form of the disease typically lack a family history of PD. Understanding different forms of PD is crucial for developing targeted therapies for affected individuals.

Transcriptomic analyses have provided transformative insights into molecular mechanisms underlying PD. Studies have revealed dysregulated gene expression profiles in diverse sample types—including brain tissue, blood, serum exosomes, and skin—highlighting systemic molecular changes and "skin-brain" crosstalk. Notable findings include apoptosis-related gene expression alterations in the cingulate gyrus, copper metabolism-related hub genes in the substantia nigra (SN), heat shock protein dysregulation in blood samples, and complement system-associated hub genes in peripheral blood [22-30]. Single-nucleus transcriptomics has illuminated selective cell vulnerability in the prefrontal cortex, while serum exosome profiling underscores intercellular communication as a potential biomarker and therapeutic target [31,32]. Collectively, transcriptomic analyses across diverse sample types have paved the way for novel biomarkers, therapeutic targets, and a deeper understanding of the interplay between central and peripheral mechanisms in PD.

In both familial and idiopathic PD, the progressive loss of DA neurons located in SN is the defining feature of the disease. Despite the differences in their genetic basis, some common pathways and mechanisms may contribute to DA neuron degeneration in familial and idiopathic PD. Identifying the shared dysregulated genes and pathways can uncover core cellular processes contributing to DA neuron degeneration across PD forms. High-throughput RNA sequencing has been used to identify dysregulated genes by comparing gene expression patterns in healthy and PD-afflicted DA neurons [33-39]. Samples such as postmortem brain tissue and induced pluripotent stem cells (iPSC)-derived models offer unique advantages; postmortem tissue provides invaluable insights into the actual pathological state of the disease, and iPSCs offer a dynamic and renewable platform for modeling disease progression and developing therapies [33-39]. Together, these approaches enhance our understanding of PD and facilitate the development of novel therapies that could be effective for a broader population of PD patients, regardless of genetic background.

Several model organisms are employed to study PD [40]. The invertebrate *Caenorhabditis elegans* presents unique advantages, including its small size, rapid lifecycle, and cost-effective maintenance, which enable

high-throughput studies on large populations. Notably, *C. elegans* shares over 80% genetic homology with human disease-related genes and possesses DA neurons, making it an excellent platform for identifying and characterizing genes and factors involved in DA neuron degeneration [41-44]. Moreover, human α-synuclein-expressing *C. elegans* models recapitulate key PD phenotypes, such as age-dependent α-synuclein aggregation, DA neuron loss, and disruptions in DA-dependent behaviors [45-48]. Additionally, the neurotoxin 1-methyl-4-phenyl 1,2,3,6 tetrahydropyridine (MPTP)-treated SH-SY5Y is extensively employed to investigate the molecular and cellular mechanisms underlying PD pathology and to evaluate potential neuroprotective compounds for PD treatment [49-55]. Together, *C. elegans* and SH-SY5Y cells offer robust and complementary tools for uncovering the mechanisms of PD and developing potential therapeutic interventions.

In this study, we integrated datasets from Novosadova, E. et al., Zaccaria, A. et al., and Kim, J.W. et al., representing RNA sequencing of DA neurons in familial and idiopathic PD (**Graphical Abstract**) [34,35,39]. We identified 40 genes dysregulated in the DA neurons in all three databases. Analysis of the Protein-Protein Interaction (PPI) network of these genes identified 12 hub genes. Gene ontology (GO) analysis highlighted the functional roles of genes in various biological processes, molecular functions, and cellular components. Using the Reactome database, we identified enriched pathways in which the genes participate, shedding light on fundamental cellular processes related to DA neuron degeneration in PD. Our findings were validated in the *Caenorhabditis elegans* and MPTP-induced SH-SY5Y model of PD. These findings underscore the importance of shared molecular genes and pathways in PD pathogenesis and highlight dysregulated hub genes as promising candidates for therapeutic intervention.

2. Material and Methods

2.1 *In-silico* Experiments

2.1.1. Data Extraction

The data used in this study were obtained from the Gene Expression Omnibus (GEO) (http://www.ncbi.nlm.nih.gov/geo/) database [56]. The GEO database is a publicly accessible resource for functional genomic data, including microarrays, chips, and high-throughput gene expression datasets. The keyword "Parkinson's Disease" was used to search the database, and the search results were filtered for the Organism "*Homo sapiens*" and Study type "Expression profiling by high throughput sequencing." Among the filtered results, datasets meeting the following criteria were included:

1. Profiling conducted on:
    a) SN-DA neurons from post-mortem brains, or
    b) Human iPSC-derived DA neurons
2. Samples included PD and healthy controls.
3. Analysis with GEO2R is available.

Based on the inclusion criteria, three gene datasets (GSE90469, GSE169755, and GSE181029) were selected for further analysis [34,35,39]. Further information on these datasets is summarized in **Table 1**.

2.1.2. Differentially Expressed Genes (DEGs) Identification

GEO2R, an online sequencing data analysis tool developed by the GEO database, was used to analyze gene expression profiles and identify DEGs between PD and control DA neurons for each dataset. GEO2R utilizes two R packages (GEOquery and Limma) for its analyses (https://www.r-project.org) [57-59]. GEOquery reads the data, while Limma calculates differential expressions. The samples used to perform analysis in each dataset are summarised in **Table 2**. The $p \leq 0.05$ and $|\log_2$ Fold-Change (FC)$| \geq 0.5$ were set as thresholds for DEGs. Gene expression distributions for each dataset were visualized using volcano plots and box plots. Overlapping DEGs from the three datasets were defined as common DEGs (cDEGs) and displayed using Venn diagrams created with the online platform Venny 2.1.0 (http://bioinfogp.cnb.csic.es/tools/venny/index.html).

2.1.3. PPI Network Analysis

A PPI network of the proteins encoded by the cDEGs was predicted and constructed using the GeneMANIA plugin of Cytoscape software (version: 3.8.0; http://cyto-scape.org/) [60]. The minimum required interaction score for the PPI analysis was set at a combined score ≥ 0.4. Nodes represented proteins, while edges denoted interactions between proteins. The Molecular Complex Detection (MCODE) plugin in Cytoscape was employed to perform network clustering analysis to identify key functional modules. These modules represent groups of highly interconnected proteins within the PPI network, suggesting they may participate in related biological pathways critical to DA neuron function and survival. The selection criteria for clustering included K-core = 2, degree cutoff = 2, max depth = 100, and node score cutoff = 0.2. Significant modules identified through MCODE analysis were used to identify hub genes.

2.1.4. Functional Enrichment Analysis

Functional enrichment analysis of GO terms was conducted using the Database for Annotation, Visualization, and Integrated Discovery (DAVID) (https://david.ncifcrf.gov/) [61]. Significantly enriched function annotations were defined as GO terms and Reactome pathways with $p \leq 0.05$. GO analysis included biological processes, cellular components, and molecular functions to describe the activity and localization of genes. The bubble plots of GO terms and Reactome pathways were visualized via the "ggplot2" package of RStudio software (version 1.3.959; https://rstudio.com/) [62].

2.1.5. Gene-Disease Association Analysis

Diseases often share genetic underpinnings, with some genes implicated in multiple disorders. Understanding these gene-disease associations can provide insights into the broader implications of gene dysregulation beyond PD. Gene-disease associations were studied using the DisGeNET database

integrated into the NetworkAnalyst platform. DisGeNET aggregates data from sources like GWAS catalogs and literature collections, facilitating insights into genetic underpinnings and comorbidities of diseases [63].

2.2. Cell-culture Experiments

2.2.1. Cell Culture Maintenance

The human neuroblastoma cell line SH-SY5Y (ATCC) was cultured in Dulbecco's Modified Eagle Medium (Gibco™) supplemented with 10% fetal bovine serum (Gibco™) and 1% penicillin-streptomycin (Gibco™). Cells were maintained in a humidified incubator at 37°C and 5% CO_2 [64].

2.2.2. MPTP Treatment

A 10 mM stock solution of MPTP (Sigma-Aldrich) was prepared in dimethyl sulfoxide (DMSO; Sigma-Aldrich). When the cells were 80% confluent, 10^6 cells/ well were added to a 6-well plate. MPTP was diluted in cell media, and the cells were exposed to MPTP at a final concentration of 200 µM for 24 h. Cells treated with 0.1% DMSO were used as control [65].

2.2.3. RNA Isolation and Quantitative Reverse Transcription Polymerase Chain Reaction (qRT-PCR)

RNA was isolated using the RNeasy Mini Kit (Qiagen). About 2µg of RNA was reverse-transcribed into cDNA with the cDNA Reverse Transcription Kit (Promega). qRT-PCR was performed using SYBR Premix Ex Taq™ (TaKaRa Bio Inc.) and RT-PCR machine (Biorad-CFX96). Gene expression levels were normalized to *GAPDH* and evaluated using the $2^{-\Delta\Delta Ct}$ method. All the primers used for the analysis are listed in **Supplementary Table 1**.

2.3. *C. elegans* Experiments

2.3.1. *C. elegans* Strains and Maintenance

The strains BY250 (P_{dat-1}::GFP) and UA44 (P_{dat-1}::GFP, P_{dat-1}:: human-α-synuclein^{wt}) were procured from *Caenorhabditis Genetics Center* (CGC), University of Minnesota, MN, USA, and maintained on the nematode growth medium (NGM) plate seeded with *Escherichia. coli* OP50 as the maintenance food at 20°C [66]. Adult worms were treated with a bleaching solution to isolate eggs, which were then age-synchronized at the first larval stage (L1) in M9 buffer at 20°C for 16-18 h [66]. The synchronized L1 larvae were subsequently transferred to NGM RNA Interference (RNAi) plates for gene knockdown experiments.

2.3.2. RNAi Induction

RNAi was performed by feeding worms with *E. coli* strain HT115 (DE3) carrying a plasmid (L4440) expressing double-stranded RNA targeting a gene of interest [67]. HT115 (DE3) carrying the empty vector was used as a control RNAi. The bacteria were cultured overnight in Luria-Bertani broth (LB) containing 100 µg/ml ampicillin (Sigma) and 12.5 µg/ml tetracycline (Sigma) at 37°C. This overnight culture was used

to inoculate fresh LB containing 100 µg/ml ampicillin in a 1:100 ratio. The secondary cultures were grown at 37°C until they reached an OD_{600} of 0.4. The cultures were then centrifuged, and the pellets were resuspended in M9 buffer containing 1mM isopropyl β-D-1-thiogalactopyranoside (IPTG) (Sigma) and 100 µg/ml ampicillin. 400 µl of the resuspended culture was used to plate 60 mm NGM plates supplemented with 100 µg/ml ampicillin and 2mM IPTG. The seeded plates were left in a laminar hood for 16 h and then stored at 4°C until L1-stage worms were transferred onto the RNAi plates. To prevent progeny growth, 40 µM fluoro-2'-deoxy-β-uridine (TCI) was added at the fourth larval stage [68].

2.3.3. DA Neuron Imaging

Three-day-old adult worms were collected from RNAi plates, washed with M9 buffer, and transferred onto a 2% agarose pad on a glass slide. The worms were anesthetized with 30 mM sodium azide (Sigma) and covered with a coverslip. Images of the head region were captured at 20X magnification using a fluorescence microscope (Carl Zeiss), and the fluorescence intensity of GFP in DA neurons was quantified using ImageJ software (NIH, Bethesda, MD) [69]. A minimum of 20 worms were imaged for each RNAi experiment.

2.3.4. RNA Isolation and qRT-PCR

Worms at day three of adulthood were collected and washed with M9 buffer. Trizol reagent (Invitrogen™) was added at approximately four times the volume of the worm pellet, and the worms were lysed through two freeze-thaw cycles followed by vigorous vortexing. RNA was purified using phenol:chloroform: isoamyl alcohol extraction and isopropanol precipitation [70]. qRT-PCR was performed following the protocol described in section 2.2.4, with gene expression levels normalized to β-actin and analyzed using the $2^{-\Delta\Delta Ct}$ method [70]. The primers used for the analysis are listed in **Supplementary Table 1**.

2.4. Statistical Analysis of Cells and *C. elegans* Experiments

Statistical analysis was conducted using GraphPad Prism 8 software (GraphPad, Inc., La Jolla, CA, United States). Data were expressed as mean ± standard deviation, and statistical significance was evaluated using Student's t-test, with $p \leq 0.05$ considered statistically significant.

3. Results

3.1. Identification of cDEGs among the datasets GSE90469, GSE169755, and GSE181029

GEO2R analysis of GSE90469 identified 1,384 DEGs ($p \leq 0.05$ and $|\log_2 FC| > 0.5$), of which 611 were upregulated, and 773 were downregulated in iPSC-derived DA neurons from patients with *LRRK2* (G2019S)-PD compared to controls (**Figure 1A**). In GSE169755, the analysis revealed 1,995 DEGs ($p \leq 0.05$ and $|\log_2 FC| > 0.5$), of which 1,234 were upregulated, and 761 were downregulated in DA neurons isolated from the SN of idiopathic PD patients as compared to controls (**Figure 1A**). From the GSE181029 dataset, 5,501 DEGs ($p \leq 0.05$ and $|\log_2 FC| > 0.5$) were identified, of which 2,843 were upregulated, and

2,658 were downregulated in iPSC-derived DA neurons from patients with three different *PARK2* mutations (**Figure 1A**). Gradient volcano plots illustrating the distribution of DEGs in each dataset are shown in **Figure 1B**. A Venn diagram revealed that 21 genes were upregulated and 19 were down-regulated in all three datasets (Fig. 1C-E). The identification of 40 cDEGs suggests a mechanistic contribution to PD pathogenesis, highlighting candidates for in-depth mechanistic studies into neurodegenerative processes.

3.2. Generation of PPI Network of cDEGs

The PPI network of cDEGs, constructed using Cytoscape based on the GeneMANIA database, included 58 nodes and 326 edges (**Figure 2A**). The MCODE plugin was applied to identify significant clusters or "modules" within the network. The analysis revealed three significant modules: Module 1 contained 17 nodes and 71 edges, Module 2 contained four nodes and nine edges, and Module 3 contained three nodes and six edges (**Figure 2B**). The nodes in these three modules included 12 cDEGs- *CELF3, PHF11, RAB6B, ADGRB3, BTN3A2, GRIA1, HCN4, KIF3C, PSMB8, RGS8, SEPTIN3,* and *SAMD14*. These 12 cDEGs were identified as hub genes, representing the most highly interconnected nodes within the network.

3.3. Functional Enrichment

We performed GO analysis of the hub genes to identify key functional and pathway associations potentially driving DA neuron degeneration in familial and idiopathic PD. The analysis revealed two significant molecular functions (myosin V binding and GTPase activity) and three significant cellular components (dendrite, presynapse, and neuronal cell body membrane) (**Figure 2C**, **Table 3**). However, for biological processes, the GO analysis resulted in two non-significant biological processes (calcium-mediated signaling and neuron projection development). Pathway analysis through Reactome indicated that the hub genes involved membrane trafficking and vesicle-mediated transport (**Figure 2C**, **Table 3**). These findings suggest that hub genes, by regulating various critical functions, may play a pivotal role in the degeneration of DA neurons in familial and idiopathic PD.

3.4. Hub Gene-Disease Associations

The hub gene-disease network analysis identified four distinct subnetworks. Subnetwork 1 comprised the hub gene *PSMB8* and its association with 83 diseases (**Figure 3A**). Subnetwork 2 linked *GRIA1* to 13 diseases (**Figure 3B**), while Subnetwork 3 connected *HCN4* to 10 diseases (**Figure 3C**). The Subnetwork 4 showed an association between *PHF11* and two diseases (**Figure 3D**). Together, these subnetworks illustrate the varied disease associations of key hub genes, underscoring their potential roles in disease pathogenesis.

3.5. Validation of hub genes in the SH-SY5Y model of PD

We validated the expression patterns of the identified hub genes in an *in vitro* PD model using the neurotoxin MPTP-treated SH-SY5Y human neuroblastoma cells. qRT-PCR analysis demonstrated that,

among the upregulated hub genes, *PSMB8* (2.03 ± 0.37; $p < 0.04$) and *BTN3A2* (1.66 ± 0.21; $p < 0.04$) exhibited significantly elevated expression levels in MPTP-treated SH-SY5Y cells compared to untreated controls (**Figure 4A**). Conversely, for the downregulated hub genes, qRT-PCR results revealed significantly decreased expression levels of *RGS8* (0.38 ± 0.14; $p < 0.02$), *CELF3* (0.39 ± 0.09; $p < 0.003$), *RAB6B* (0.74 ± 0.06; $p < 0.02$), *SEPTIN3* (0.57 ± 0.07; $p < 0.005$), and *HCN4* (0.42 ± 0.08; $p < 0.002$) in MPTP-treated cells relative to controls (**Figure 4B**). Overall, these results validate the differential expression of the identified hub genes in an *in vitro* PD model, reinforcing their potential significance in PD pathology.

3.6. *Rgs8* RNAi degenerates DA neurons in healthy *C. elegans*

The altered expression of the validated hub genes suggests they may play critical roles in maintaining DA neuron health. To test this hypothesis, we employed the *C. elegans* model, using the feeding RNAi method to investigate the functional significance of these hub genes. We first sought to determine which of the hub genes validated in MPTP-treated SH-SY5Y cells also exhibit altered expression in the nematode PD model UA44, which expresses human α-synuclein and GFP specifically in DA neurons. We used the BY250 strain as a healthy control, which expresses GFP in DA neurons but lacks α-synuclein expression. Both strains were fed control (empty vector) RNAi, and fluorescence microscopy performed at day 3 of adulthood revealed a significant reduction in fluorescence intensity in DA neurons of UA44 worms (9.47 ± 0.58, $p < 0.0001$) compared to BY250 worms (21.42 ± 1.14) (**Figure 5A and B**), confirming DA neuron degeneration in the PD model.

Subsequently, qRT-PCR analysis demonstrated a significant reduction in the mRNA levels of the *rgs8* homolog, *C29H12.3*, in UA44 worms (0.55 ± 0.13, $p < 0.03$) relative to BY250 controls (**Figure 5C**), suggesting a potential role for *C29H12.3/rgs8* in DA neurodegeneration. To further investigate this, we performed RNAi-mediated knockdown of *C29H12.3/rgs8* in BY250 worms and evaluated its impact on DA neuron integrity. qRT-PCR confirmed efficient knockdown, with a significant reduction in *C29H12.3/rgs8* mRNA levels (0.23 ± 0.04, $p < 0.0001$) in *C29H12.3/rgs8* RNAi-fed worms compared to control RNAi-fed worms (**Figure 5C**). Consistent with a role in neuronal maintenance, fluorescence microscopy at day 3 of adulthood revealed a significant decrease in fluorescence intensity in DA neurons of *C29H12.3/rgs8* RNAi-treated BY250 worms (15.81 ± 1.15, $p < 0.002$) compared to controls (21.42 ± 1.14) (**Figure 5A and B**). These results suggest that *C29H12.3/rgs8* is essential for maintaining DA neuron integrity and may contribute to the molecular mechanisms underlying neurodegeneration in PD.

4. Discussion

This study offers valuable insights into the shared molecular mechanisms underlying DA neuron degeneration in familial and idiopathic PD forms. Previous research has demonstrated the utility of reanalyzing publicly available transcriptomic datasets to uncover novel biological insights [71-78]. In this study, we integrated RNA sequencing data from three independent datasets, each representing distinct genetic and pathological contexts of PD. Through this approach, we identified 40 cDEGs, including 12 hub genes, which may play key roles in the pathogenesis of PD. Functional enrichment analysis revealed that hub

genes participate in pathways essential for maintaining neuronal health and synaptic integrity—disrupted processes in PD.

Although the datasets represent samples with differing genetic backgrounds—potentially influencing disease onset and progression—our aim was to identify converging molecular alterations that may represent shared pathogenic mechanisms across PD subtypes. The identification and subsequent experimental validation of these genes underscore the existence of common molecular disruptions in familial and idiopathic PD, highlighting potential targets for therapeutic intervention.

Notably, several of the cDEGs identified in our analysis, including *PPP1R1B*, *DEPTOR*, *DLGAP3*, *GJA1*, *IL13RA1*, *LIPA*, *NECAB1*, and *PSMB8*, have previously been reported to exhibit altered expression in PD models and human PD brain tissues [79-104]. Although these prior studies primarily focused on idiopathic PD, our findings extend the relevance of these genes by demonstrating their dysregulation across both idiopathic and familial PD datasets, suggesting that their involvement in DA neuron degeneration may represent a common molecular signature of PD independent of genetic origin.

The hub genes, *PSMB8, GRIA1,* and *RGS8,* exhibit expression changes consistent with previous reports, supporting their potential relevance to PD pathophysiology [105-107]. In addition, our study demonstrates that *rgs8* mRNA levels are significantly reduced not only in the MPTP-treated SH-SY5Y cell model of PD but also in the transgenic *C. elegans* PD model, complementing earlier findings of reduced *rgs8* expression in the rat α-synuclein preformed fibril model [107]. Notably, this is the first study to show, using the *C. elegans* model, that *rgs8* downregulation leads to DA neurodegeneration. RGS8 (Regulator of G Protein Signaling 8) is known to regulate G protein-coupled receptor (GPCR) signaling by acting as a GTPase-activating protein [108]. Given that GPCRs are essential to dopamine signaling, RGS8 may be crucial in maintaining DA neuron health [109]. Future studies should aim to elucidate the molecular mechanisms by which *rgs8* regulates DA neuron integrity and its potential contribution to PD progression.

The other hub genes are linked to DA neuron dysfunction in PD for the first time in this study (**Table 4**). For example, *BTN3A2*, a member of the butyrophilin subfamily, is primarily known for its role in modulating immune responses [110]. Since neuroinflammation is a well-established contributor to PD pathogenesis, the upregulation of BTN3A2 observed in PD-DA neurons suggests a potential link between peripheral immune signaling and central neurodegenerative processes in idiopathic and familial PD [111]. Similarly, *HCN4* (Hyperpolarization-Activated Cyclic Nucleotide-Gated Potassium Channel 4), which modulates neuronal excitability via potassium channel regulation, also emerged as a downregulated hub gene. Alterations in *HCN4* expression may impair neuronal membrane potentials and contribute to excitotoxicity—a well-documented mechanism of neurodegeneration in PD [112,113]. Together, these findings highlight the previously unrecognized involvement of several genes in DA neuron degeneration and suggest that these hub genes may represent critical molecular nodes in PD pathogenesis. Further mechanistic studies are needed to elucidate their functional roles and therapeutic potential.

Genes play a central role in regulating a wide array of cellular functions, and disruptions in their expression can perturb essential biological pathways, thereby contributing to the development and progression of various diseases. Our gene-disease network analysis revealed one of the hub genes, *GRIA1,* with established associations with bipolar disorder—a neuropsychiatric condition marked by altered DA signaling during manic and depressive phases [114,115]. Notably, emerging evidence suggests that individuals with bipolar disorder may be at an elevated risk of developing PD later in life [116]. Although polymorphisms in *GRIA1* have been linked to psychotic subtypes of bipolar disorder, their specific role in PD pathogenesis remains undefined and merits further investigation [117]. Uncovering shared genetic contributors such as *GRIA1* across distinct neurological disorders holds promise for developing therapeutic strategies that target convergent molecular mechanisms.

Collectively, these findings strengthen the case for shared molecular pathways across familial and idiopathic PD forms and provide a foundation for future research into therapeutic targeting of hub genes. Given the limitations of existing PD treatments—largely symptomatic and failing to halt disease progression—targeting common pathogenic mechanisms may offer broader clinical benefits.

However, several limitations of this study warrant consideration. First, the reliance on transcriptomic data captures only one layer of gene regulation, and additional studies incorporating proteomic, epigenetic, and metabolomic data could provide a more comprehensive view. Second, while SH-SY5Y and *C. elegans* models are powerful for validation, they do not fully replicate the complexity of human DA neurons and brain architecture. Further *in vivo* validation in mammalian models, such as mice or non-human primates, is necessary to confirm the translational relevance of the findings. Finally, the functional roles of many hub genes remain poorly understood, and in-depth mechanistic studies will be essential to elucidate their contributions to DA neuron vulnerability.

Nevertheless, our study provides valuable insights into the DA neuron-specific shared molecular mechanisms underlying familial and idiopathic PD. These findings expand the landscape of molecular players in PD pathogenesis, providing new hypotheses for experimental validation. We hope that the findings from our study will inspire future experimental validation, fostering new insights into shared molecular mechanisms and uncovering novel therapeutic targets to deepen our understanding of PD.

Acknowledgments

S is supported by Senior Research Fellowship from CSIR. GC is supported by Junior Research Fellowship UGC. We thank the Director of CSIR-CDRI for providing the necessary research facilities. We sincerely thank the faculty members of the Division of Neuroscience and Ageing Biology, CSIR-CDRI, for providing access to the cell culture facility and the RT-PCR machine (Biorad-CFX96). We would also like to acknowledge Dr. Aamir Nazir, Division of Toxicology & Experimental Medicine, CSIR-CDRI, for sharing *C29H12.3/rgs8* RNAi and providing access to the fluorescence microscope (Carl Zeiss).

CRediT authorship contribution statement

S- Investigation; Data curation; Methodology; Writing—original draft; Writing—review and editing.

GC- Investigation; Methodology; Writing—original draft.

BM- Resources; Investigation. Writing - review & editing.

SV- Conceptualization; Investigation; Data curation; Formal analysis; Methodology; Project administration; Resources; Supervision; Validation; Visualization; Writing - original draft; and Writing - review & editing.

Declaration of interest

The authors declare that they have no known competing financial interests or personal relationships that could have appeared to influence the work reported in this paper.

Data Availability

The datasets used in this study are available in the GEO database [https://www.ncbi.nlm.nih. gov/geo/]. Details about the corresponding accession numbers are provided within the article.

Funding Source

The work is supported by start-up funding from Director CSIR-CDRI to SV.

References

1 Maiti, P., Manna, J. & Dunbar, G. L. Current understanding of the molecular mechanisms in Parkinson's disease: Targets for potential treatments. *Transl Neurodegener* **6**, 28, doi:10.1186/s40035-017-0099-z (2017).

2 Rizek, P., Kumar, N. & Jog, M. S. An update on the diagnosis and treatment of Parkinson disease. *CMAJ* **188**, 1157-1165, doi:10.1503/cmaj.151179 (2016).

3 Eisbach, S. E. & Outeiro, T. F. Alpha-synuclein and intracellular trafficking: impact on the spreading of Parkinson's disease pathology. *J Mol Med (Berl)* **91**, 693-703, doi:10.1007/s00109-013-1038-9 (2013).

4 Xu, L. & Pu, J. Alpha-Synuclein in Parkinson's Disease: From Pathogenetic Dysfunction to Potential Clinical Application. *Parkinsons Dis* **2016**, 1720621, doi:10.1155/2016/1720621 (2016).

5 Zhang, Y. *et al.* A Comprehensive Analysis of the Association Between SNCA Polymorphisms and the Risk of Parkinson's Disease. *Front Mol Neurosci* **11**, 391, doi:10.3389/fnmol.2018.00391 (2018).

6 Zhu, C., Herbst, S. & Lewis, P. A. Leucine-rich repeat kinase 2 at a glance. *J Cell Sci* **136**, doi:10.1242/jcs.259724 (2023).

7 Lee, J. W. & Cannon, J. R. LRRK2 mutations and neurotoxicant susceptibility. *Exp Biol Med (Maywood)* **240**, 752-759, doi:10.1177/1535370215579162 (2015).

8 Kluss, J. H., Mamais, A. & Cookson, M. R. LRRK2 links genetic and sporadic Parkinson's disease. *Biochem Soc Trans* **47**, 651-661, doi:10.1042/BST20180462 (2019).

9 Pickrell, A. M. & Youle, R. J. The roles of PINK1, parkin, and mitochondrial fidelity in Parkinson's disease. *Neuron* **85**, 257-273, doi:10.1016/j.neuron.2014.12.007 (2015).

10 Fiesel, F. C. *et al.* Structural and Functional Impact of Parkinson Disease-Associated Mutations in the E3 Ubiquitin Ligase Parkin. *Hum Mutat* **36**, 774-786, doi:10.1002/humu.22808 (2015).

11 Fang, Y. Q., Mao, F., Zhu, M. J. & Li, X. H. Compound heterozygous mutations in PARK2 causing early-onset Parkinson disease: A case report. *Medicine (Baltimore)* **98**, e14228, doi:10.1097/MD.0000000000014228 (2019).

12 Dolgacheva, L. P., Berezhnov, A. V., Fedotova, E. I., Zinchenko, V. P. & Abramov, A. Y. Role of DJ-1 in the mechanism of pathogenesis of Parkinson's disease. *J Bioenerg Biomembr* **51**, 175-188, doi:10.1007/s10863-019-09798-4 (2019).
13 Skou, L. D., Johansen, S. K., Okarmus, J. & Meyer, M. Pathogenesis of DJ-1/PARK7-Mediated Parkinson's Disease. *Cells* **13**, doi:10.3390/cells13040296 (2024).
14 Siuda, J. *et al.* Early-onset Parkinson's disease due to PINK1 p.Q456X mutation--clinical and functional study. *Parkinsonism Relat Disord* **20**, 1274-1278, doi:10.1016/j.parkreldis.2014.08.019 (2014).
15 Yunfu, W. *et al.* PINK1 and its familial Parkinson's disease-associated mutation regulate brain vascular endothelial inflammation. *J Mol Neurosci* **53**, 109-116, doi:10.1007/s12031-013-0207-1 (2014).
16 Choong, C. J. & Mochizuki, H. Involvement of Mitochondria in Parkinson's Disease. *Int J Mol Sci* **24**, doi:10.3390/ijms242317027 (2023).
17 Smith, L. & Schapira, A. H. V. GBA Variants and Parkinson Disease: Mechanisms and Treatments. *Cells* **11**, doi:10.3390/cells11081261 (2022).
18 Avenali, M., Blandini, F. & Cerri, S. Glucocerebrosidase Defects as a Major Risk Factor for Parkinson's Disease. *Front Aging Neurosci* **12**, 97, doi:10.3389/fnagi.2020.00097 (2020).
19 Padhan, P., Simran, Kumar, N. & Verma, S. Glutathione S-transferase: A keystone in Parkinson's disease pathogenesis and therapy. *Mol Cell Neurosci*, 103981, doi:10.1016/j.mcn.2024.103981 (2024).
20 Grover, S. *et al.* Genome-wide Association and Meta-analysis of Age at Onset in Parkinson Disease: Evidence From the COURAGE-PD Consortium. *Neurology* **99**, e698-e710, doi:10.1212/WNL.0000000000200699 (2022).
21 Karimi-Moghadam, A., Charsouei, S., Bell, B. & Jabalameli, M. R. Parkinson Disease from Mendelian Forms to Genetic Susceptibility: New Molecular Insights into the Neurodegeneration Process. *Cell Mol Neurobiol* **38**, 1153-1178, doi:10.1007/s10571-018-0587-4 (2018).
22 Wang, Z. *et al.* Multi-omics analysis reveals the genetic aging landscape of Parkinson's disease. *Sci Rep* **14**, 31167, doi:10.1038/s41598-024-82470-z (2024).
23 Ma, L. *et al.* Integrating bioinformatics and machine learning to uncover lncRNA LINC00269 as a key regulator in Parkinson's disease via pyroptosis pathways. *Eur J Med Res* **29**, 582, doi:10.1186/s40001-024-02201-y (2024).
24 Lin, J. *et al.* Identification of copper metabolism-related markers in Parkinson's disease. *Ann Med* **56**, 2425064, doi:10.1080/07853890.2024.2425064 (2024).
25 Cheng, H. *et al.* Deciphering the role of heat shock protein HSPA1L: biomarker discovery and prognostic insights in Parkinson's disease and glioma. *SLAS Technol* **29**, 100212, doi:10.1016/j.slast.2024.100212 (2024).
26 Peng, H., Cheng, Y., Chen, Q. & Qin, L. Integrated Transcriptomic and Machine Learning Analysis Identifies EAF2 as a Diagnostic Biomarker and Key Pathogenic Factor in Parkinson's Disease. *Int J Gen Med* **17**, 5547-5562, doi:10.2147/IJGM.S486214 (2024).
27 Beric, A. *et al.* Circulating blood circular RNA in Parkinson's Disease; from involvement in pathology to diagnostic tools in at-risk individuals. *NPJ Parkinsons Dis* **10**, 222, doi:10.1038/s41531-024-00839-3 (2024).
28 Lyu, Q., Chen, R., Qiu, Z., Wang, C. & Liu, R. Druggable targets for Parkinson's disease: transcriptomics based Mendelian randomization study. *Sci Rep* **14**, 25763, doi:10.1038/s41598-024-77401-x (2024).
29 Wang, X., Yang, G., Lai, Y., Li, Y. & Liu, X. Exploring the hub Genes and Potential Mechanisms of Complement system-related Genes in Parkinson Disease: Based on Transcriptome Sequencing and Mendelian Randomization. *J Mol Neurosci* **74**, 95, doi:10.1007/s12031-024-02272-w (2024).
30 Planken, A. *et al.* Looking beyond the brain to improve the pathogenic understanding of Parkinson's disease: implications of whole transcriptome profiling of Patients' skin. *BMC Neurol* **17**, 6, doi:10.1186/s12883-016-0784-z (2017).
31 Yu, Z. *et al.* Comprehensive data for studying serum exosome microRNA transcriptome in Parkinson's disease patients. *Sci Data* **11**, 1128, doi:10.1038/s41597-024-03909-6 (2024).
32 Zhu, B. *et al.* Single-cell transcriptomic and proteomic analysis of Parkinson's disease brains. *Sci Transl Med* **16**, eabo1997, doi:10.1126/scitranslmed.abo1997 (2024).
33 Kamath, T. *et al.* Single-cell genomic profiling of human dopamine neurons identifies a population that selectively degenerates in Parkinson's disease. *Nat Neurosci* **25**, 588-595, doi:10.1038/s41593-022-01061-1 (2022).
34 Novosadova, E. *et al.* Transcriptome datasets of neural progenitors and neurons differentiated from induced pluripotent stem cells of healthy donors and Parkinson's disease patients with mutations in the PARK2 gene. *Data Brief* **41**, 107958, doi:10.1016/j.dib.2022.107958 (2022).

35 Zaccaria, A. *et al.* Multiomic Analyses of Dopaminergic Neurons Isolated from Human Substantia Nigra in Parkinson's Disease: A Descriptive and Exploratory Study. *Cell Mol Neurobiol* **42**, 2805-2818, doi:10.1007/s10571-021-01146-8 (2022).
36 Fernandez-Santiago, R. *et al.* Aberrant epigenome in iPSC-derived dopaminergic neurons from Parkinson's disease patients. *EMBO Mol Med* **7**, 1529-1546, doi:10.15252/emmm.201505439 (2015).
37 Aguila, J. *et al.* Spatial RNA Sequencing Identifies Robust Markers of Vulnerable and Resistant Human Midbrain Dopamine Neurons and Their Expression in Parkinson's Disease. *Front Mol Neurosci* **14**, 699562, doi:10.3389/fnmol.2021.699562 (2021).
38 Drouin-Ouellet, J. *et al.* Age-related pathological impairments in directly reprogrammed dopaminergic neurons derived from patients with idiopathic Parkinson's disease. *Stem Cell Reports* **17**, 2203-2219, doi:10.1016/j.stemcr.2022.08.010 (2022).
39 Kim, J. W. *et al.* Defects in mRNA Translation in LRRK2-Mutant hiPSC-Derived Dopaminergic Neurons Lead to Dysregulated Calcium Homeostasis. *Cell Stem Cell* **27**, 633-645 e637, doi:10.1016/j.stem.2020.08.002 (2020).
40 Khan, E., Hasan, I. & Haque, M. E. Parkinson's Disease: Exploring Different Animal Model Systems. *Int J Mol Sci* **24**, doi:10.3390/ijms24109088 (2023).
41 Lai, C. H., Chou, C. Y., Ch'ang, L. Y., Liu, C. S. & Lin, W. Identification of novel human genes evolutionarily conserved in Caenorhabditis elegans by comparative proteomics. *Genome Res* **10**, 703-713, doi:10.1101/gr.10.5.703 (2000).
42 Gaeta, A. L., Caldwell, K. A. & Caldwell, G. A. Found in Translation: The Utility of C. elegans Alpha-Synuclein Models of Parkinson's Disease. *Brain Sci* **9**, doi:10.3390/brainsci9040073 (2019).
43 Pingale, T. & Gupta, G. L. Classic and evolving animal models in Parkinson's disease. *Pharmacol Biochem Behav* **199**, 173060, doi:10.1016/j.pbb.2020.173060 (2020).
44 Cooper, J. F. & Van Raamsdonk, J. M. Modeling Parkinson's Disease in C. elegans. *J Parkinsons Dis* **8**, 17-32, doi:10.3233/JPD-171258 (2018).
45 Di Rosa, G. *et al.* Healthspan Enhancement by Olive Polyphenols in C. elegans Wild Type and Parkinson's Models. *Int J Mol Sci* **21**, doi:10.3390/ijms21113893 (2020).
46 Vijayan, B., Raj, V., Nandakumar, S., Kishore, A. & Thekkuveettil, A. Spermine protects alpha-synuclein expressing dopaminergic neurons from manganese-induced degeneration. *Cell Biol Toxicol* **35**, 147-159, doi:10.1007/s10565-018-09449-1 (2019).
47 Liang, Q. & Zhao, G. The Effect of glna Loss on the Physiological and Pathological Phenotype of Parkinson's Disease C. elegans. *J Clin Lab Anal* **38**, e25129, doi:10.1002/jcla.25129 (2024).
48 Ferreyra, M. R. *et al.* Ferrostatin-1 mitigates cellular damage in a ferroptosis-like environment in Caenorhabditis elegans. *Toxicol Sci* **200**, 357-368, doi:10.1093/toxsci/kfae066 (2024).
49 Xicoy, H., Wieringa, B. & Martens, G. J. The SH-SY5Y cell line in Parkinson's disease research: a systematic review. *Mol Neurodegener* **12**, 10, doi:10.1186/s13024-017-0149-0 (2017).
50 Kato, Y. *et al.* Cytoprotective effect of melatonin against MPP(+) toxicity in SH-SY5Y cells: Role sharing of two types of antioxidative activities of melatonin. *Biochem Biophys Res Commun* **742**, 151074, doi:10.1016/j.bbrc.2024.151074 (2025).
51 Chakkittukandiyil, A. *et al.* Synthesis and evaluation of novel ethyl ferulate derivatives as potent Keap1 inhibitors to activate the Nrf2/ARE pathway in Parkinson's disease. *Toxicol Appl Pharmacol* **494**, 117172, doi:10.1016/j.taap.2024.117172 (2025).
52 Liu, Y. *et al.* TMEM106B knockdown exhibits a neuroprotective effect in Parkinson's disease models via regulating autophagy-lysosome pathway. *Biochim Biophys Acta Mol Basis Dis* **1871**, 167553, doi:10.1016/j.bbadis.2024.167553 (2025).
53 Yang, J. T., Kuo, Y. C., Lee, K. C., De, S. & Chen, Y. Y. Resveratrol and ceftriaxone encapsulated in hybrid nanoparticles to prevent dopaminergic neurons from degeneration for Parkinson's disease treatment. *Biomater Adv* **166**, 214065, doi:10.1016/j.bioadv.2024.214065 (2025).
54 Dong-Chen, X., Yong, C., Yang, X., Chen-Yu, S. & Li-Hua, P. Signaling pathways in Parkinson's disease: molecular mechanisms and therapeutic interventions. *Signal Transduct Target Ther* **8**, 73, doi:10.1038/s41392-023-01353-3 (2023).
55 Langston, J. W. The MPTP Story. *J Parkinsons Dis* **7**, S11-S19, doi:10.3233/JPD-179006 (2017).
56 Clough, E. & Barrett, T. The Gene Expression Omnibus Database. *Methods Mol Biol* **1418**, 93-110, doi:10.1007/978-1-4939-3578-9_5 (2016).
57 Gentleman, R. C. *et al.* Bioconductor: open software development for computational biology and bioinformatics. *Genome Biol* **5**, R80, doi:10.1186/gb-2004-5-10-r80 (2004).

58 Davis, S. & Meltzer, P. S. GEOquery: a bridge between the Gene Expression Omnibus (GEO) and BioConductor. *Bioinformatics* **23**, 1846-1847, doi:10.1093/bioinformatics/btm254 (2007).
59 Smyth, G. K. Linear models and empirical bayes methods for assessing differential expression in microarray experiments. *Stat Appl Genet Mol Biol* **3**, Article3, doi:10.2202/1544-6115.1027 (2004).
60 Shannon, P. *et al.* Cytoscape: a software environment for integrated models of biomolecular interaction networks. *Genome Res* **13**, 2498-2504, doi:10.1101/gr.1239303 (2003).
61 Dennis, G., Jr. *et al.* DAVID: Database for Annotation, Visualization, and Integrated Discovery. *Genome Biol* **4**, P3 (2003).
62 Kolberg, L., Raudvere, U., Kuzmin, I., Vilo, J. & Peterson, H. gprofiler2 -- an R package for gene list functional enrichment analysis and namespace conversion toolset g:Profiler. *F1000Res* **9**, doi:10.12688/f1000research.24956.2 (2020).
63 Pinero, J. *et al.* DisGeNET: a comprehensive platform integrating information on human disease-associated genes and variants. *Nucleic Acids Res* **45**, D833-D839, doi:10.1093/nar/gkw943 (2017).
64 Ioghen, O. C., Ceafalan, L. C. & Popescu, B. O. SH-SY5Y Cell Line In Vitro Models for Parkinson Disease Research-Old Practice for New Trends. *J Integr Neurosci* **22**, 20, doi:10.31083/j.jin2201020 (2023).
65 Nguyen, H. A. T. *et al.* Antioxidant, neuroprotective, and neuroblastoma cells (SH-SY5Y) differentiation effects of melanins and arginine-modified melanins from Daedaleopsis tricolor and Fomes fomentarius. *BMC Biotechnol* **24**, 89, doi:10.1186/s12896-024-00918-6 (2024).
66 Brenner, S. The genetics of Caenorhabditis elegans. *Genetics* **77**, 71-94, doi:10.1093/genetics/77.1.71 (1974).
67 Kamath, R. S. *et al.* Systematic functional analysis of the Caenorhabditis elegans genome using RNAi. *Nature* **421**, 231-237, doi:10.1038/nature01278 (2003).
68 Zhang, Z. *et al.* Jujubae Fructus extract prolongs lifespan and improves stress tolerance in Caenorhabditis elegans dependent on DAF-16/SOD-3. *Sci Rep* **14**, 13713, doi:10.1038/s41598-024-64045-0 (2024).
69 Collins, T. J. ImageJ for microscopy. *Biotechniques* **43**, 25-30, doi:10.2144/000112517 (2007).
70 Verma, S., Jagtap, U., Goyala, A. & Mukhopadhyay, A. A novel gene-diet pair modulates C. elegans aging. *PLoS Genet* **14**, e1007608, doi:10.1371/journal.pgen.1007608 (2018).
71 Yang, Z. C. *et al.* Identification and validation of biomarkers related to mitochondria during ex vivo lung perfusion for lung transplants based on machine learning algorithm. *Gene* **936**, 149097, doi:10.1016/j.gene.2024.149097 (2025).
72 Zhu, J. *et al.* Integration of bioinformatics and multi-layered experimental validation reveals novel functions of acetylation-related genes in intervertebral disc degeneration. *Gene* **933**, 148974, doi:10.1016/j.gene.2024.148974 (2025).
73 Huang, L. *et al.* A nomoscore of four genes for predicting the rupture risk in abdominal aortic aneurysm patients with osteoarthritis. *Gene* **931**, 148877, doi:10.1016/j.gene.2024.148877 (2024).
74 Huang, J. *et al.* Identification of key mitochondria-related genes and their potential crosstalk role with immune pattern in Idiopathic pulmonary fibrosis. *Gene* **930**, 148840, doi:10.1016/j.gene.2024.148840 (2024).
75 Ke, J. *et al.* Integrated bioinformatic analysis and experimental validation for exploring the key immune checkpoint of COPD. *Gene* **927**, 148711, doi:10.1016/j.gene.2024.148711 (2024).
76 Zhou, R. *et al.* Developing and experimental validating a B cell exhaustion-related gene signature to assess prognosis and immunotherapeutic response in bladder cancer. *Gene* **927**, 148634, doi:10.1016/j.gene.2024.148634 (2024).
77 Zhou, L. *et al.* Identification and preliminary validation of differently expressed genes as candidate biomarkers associated with atherosclerosis. *Gene* **915**, 148410, doi:10.1016/j.gene.2024.148410 (2024).
78 Cui, P. *et al.* Identification and validation of ferroptosis-related lncRNA signature in intervertebral disc degeneration. *Gene* **914**, 148381, doi:10.1016/j.gene.2024.148381 (2024).
79 Santini, E. *et al.* Dopamine- and cAMP-regulated phosphoprotein of 32-kDa (DARPP-32)-dependent activation of extracellular signal-regulated kinase (ERK) and mammalian target of rapamycin complex 1 (mTORC1) signaling in experimental parkinsonism. *J Biol Chem* **287**, 27806-27812, doi:10.1074/jbc.M112.388413 (2012).
80 Spigolon, G., Cavaccini, A., Trusel, M., Tonini, R. & Fisone, G. cJun N-terminal kinase (JNK) mediates cortico-striatal signaling in a model of Parkinson's disease. *Neurobiol Dis* **110**, 37-46, doi:10.1016/j.nbd.2017.10.015 (2018).
81 Tanabe, A. *et al.* A novel tyrosine kinase inhibitor AMN107 (nilotinib) normalizes striatal motor behaviors in a mouse model of Parkinson's disease. *Front Cell Neurosci* **8**, 50, doi:10.3389/fncel.2014.00050 (2014).

82 Puschban, Z. *et al.* Evidence for dopaminergic re-innervation by embryonic allografts in an optimized rat model of the Parkinsonian variant of multiple system atrophy. *Brain Res Bull* **68**, 54-58, doi:10.1016/j.brainresbull.2005.08.025 (2005).
83 Nishi, A. & Shuto, T. Potential for targeting dopamine/DARPP-32 signaling in neuropsychiatric and neurodegenerative disorders. *Expert Opin Ther Targets* **21**, 259-272, doi:10.1080/14728222.2017.1279149 (2017).
84 Ramalingam, M. *et al.* Autophagy Signaling by Neural-Induced Human Adipose Tissue-Derived Stem Cell-Conditioned Medium during Rotenone-Induced Toxicity in SH-SY5Y Cells. *Int J Mol Sci* **23**, doi:10.3390/ijms23084193 (2022).
85 Liu, S., Zhang, Y., Bian, H. & Li, X. Gene expression profiling predicts pathways and genes associated with Parkinson's disease. *Neurol Sci* **37**, 73-79, doi:10.1007/s10072-015-2360-5 (2016).
86 Jabbari, E. *et al.* Proximity extension assay testing reveals novel diagnostic biomarkers of atypical parkinsonian syndromes. *J Neurol Neurosurg Psychiatry* **90**, 768-773, doi:10.1136/jnnp-2018-320151 (2019).
87 Santaella, A. *et al.* Inflammation biomarker discovery in Parkinson's disease and atypical parkinsonisms. *BMC Neurol* **20**, 26, doi:10.1186/s12883-020-1608-8 (2020).
88 Zhao, Y. *et al.* Connexin43 inhibition attenuated dopaminergic neuronal loss in the lipopolysaccharide-induced mice model of Parkinson's disease. *Neurosci Lett* **771**, 136471, doi:10.1016/j.neulet.2022.136471 (2022).
89 Diaz, E. F. *et al.* Connexin 43 hemichannels and pannexin-1 channels contribute to the alpha-synuclein-induced dysfunction and death of astrocytes. *Glia* **67**, 1598-1619, doi:10.1002/glia.23631 (2019).
90 Kim, I. S., Ganesan, P. & Choi, D. K. Cx43 Mediates Resistance against MPP(+)-Induced Apoptosis in SH-SY5Y Neuroblastoma Cells via Modulating the Mitochondrial Apoptosis Pathway. *Int J Mol Sci* **17**, doi:10.3390/ijms17111819 (2016).
91 Phani, S., Jablonski, M., Pelta-Heller, J., Cai, J. & Iacovitti, L. Gremlin is a novel VTA derived neuroprotective factor for dopamine neurons. *Brain Res* **1500**, 88-98, doi:10.1016/j.brainres.2013.01.017 (2013).
92 Zhang, P. *et al.* Novel diagnostic biomarkers related to immune infiltration in Parkinson's disease by bioinformatics analysis. *Front Neurosci* **17**, 1083928, doi:10.3389/fnins.2023.1083928 (2023).
93 Xu, J. *et al.* Identification of key genes and signaling pathways associated with dementia with Lewy bodies and Parkinson's disease dementia using bioinformatics. *Front Neurol* **14**, 1029370, doi:10.3389/fneur.2023.1029370 (2023).
94 Aguirre, C. A. *et al.* Two single nucleotide polymorphisms in IL13 and IL13RA1 from individuals with idiopathic Parkinson's disease increase cellular susceptibility to oxidative stress. *Brain Behav Immun* **88**, 920-924, doi:10.1016/j.bbi.2020.04.007 (2020).
95 Maher, P. & Conti, B. Deciphering the pathways that protect from IL-13-mediated potentiation of oxidative stress-induced dopaminergic nerve cell death. *Cytokine* **103**, 114-120, doi:10.1016/j.cyto.2017.09.018 (2018).
96 Morrison, B. E. *et al.* Cutting edge: IL-13Ralpha1 expression in dopaminergic neurons contributes to their oxidative stress-mediated loss following chronic peripheral treatment with lipopolysaccharide. *J Immunol* **189**, 5498-5502, doi:10.4049/jimmunol.1102150 (2012).
97 Mori, S. *et al.* Lack of interleukin-13 receptor alpha1 delays the loss of dopaminergic neurons during chronic stress. *J Neuroinflammation* **14**, 88, doi:10.1186/s12974-017-0862-1 (2017).
98 Yu, M. *et al.* Functional screening of lysosomal storage disorder genes identifies modifiers of alpha-synuclein neurotoxicity. *PLoS Genet* **19**, e1010760, doi:10.1371/journal.pgen.1010760 (2023).
99 Berard, M. *et al.* A light-inducible protein clustering system for in vivo analysis of alpha-synuclein aggregation in Parkinson disease. *PLoS Biol* **20**, e3001578, doi:10.1371/journal.pbio.3001578 (2022).
100 Underwood, R. *et al.* 14-3-3 mitigates alpha-synuclein aggregation and toxicity in the in vivo preformed fibril model. *Acta Neuropathol Commun* **9**, 13, doi:10.1186/s40478-020-01110-5 (2021).
101 Ugras, S. *et al.* Induction of the Immunoproteasome Subunit Lmp7 Links Proteostasis and Immunity in alpha-Synuclein Aggregation Disorders. *EBioMedicine* **31**, 307-319, doi:10.1016/j.ebiom.2018.05.007 (2018).
102 Lee, J. A. *et al.* Activation of the Nrf2 signaling pathway and neuroprotection of nigral dopaminergic neurons by a novel synthetic compound KMS99220. *Neurochem Int* **112**, 96-107, doi:10.1016/j.neuint.2017.11.006 (2018).
103 Mo, M. S. *et al.* Association Analysis of Proteasome Subunits and Transporter Associated with Antigen Processing on Chinese Patients with Parkinson's Disease. *Chin Med J (Engl)* **129**, 1053-1058, doi:10.4103/0366-6999.180513 (2016).

104 Zhou, H. *et al.* Oxyphylla A Promotes Degradation of alpha-Synuclein for Neuroprotection via Activation of Immunoproteasome. *Aging Dis* **11**, 559-574, doi:10.14336/AD.2019.0612 (2020).
105 Nguyen, H. D. *et al.* Upregulation of immunoproteasome PSMB8 is associated with Parkinson's disease. *Parkinsonism Relat Disord* **114**, 105797, doi:10.1016/j.parkreldis.2023.105797 (2023).
106 Palasz, E. *et al.* Exercise-Induced Neuroprotection and Recovery of Motor Function in Animal Models of Parkinson's Disease. *Front Neurol* **10**, 1143, doi:10.3389/fneur.2019.01143 (2019).
107 Patterson, J. R. *et al.* Transcriptomic profiling of early synucleinopathy in rats induced with preformed fibrils. *NPJ Parkinsons Dis* **10**, 7, doi:10.1038/s41531-023-00620-y (2024).
108 O'Brien, J. B., Wilkinson, J. C. & Roman, D. L. Regulator of G-protein signaling (RGS) proteins as drug targets: Progress and future potentials. *J Biol Chem* **294**, 18571-18585, doi:10.1074/jbc.REV119.007060 (2019).
109 Gurevich, E. V., Gainetdinov, R. R. & Gurevich, V. V. G protein-coupled receptor kinases as regulators of dopamine receptor functions. *Pharmacol Res* **111**, 1-16, doi:10.1016/j.phrs.2016.05.010 (2016).
110 Lin, Y., Zhou, H. & Li, S. BTN3A2 Expression Is Connected With Favorable Prognosis and High Infiltrating Immune in Lung Adenocarcinoma. *Front Genet* **13**, 848476, doi:10.3389/fgene.2022.848476 (2022).
111 Kouli, A. *et al.* Neuroinflammation is linked to dementia risk in Parkinson's disease. *Brain* **147**, 923-935, doi:10.1093/brain/awad322 (2024).
112 Crunelli, V., David, F., Morais, T. P. & Lorincz, M. L. HCN channels and absence seizures. *Neurobiol Dis* **181**, 106107, doi:10.1016/j.nbd.2023.106107 (2023).
113 Daniel, N. H., Aravind, A. & Thakur, P. Are ion channels potential therapeutic targets for Parkinson's disease? *Neurotoxicology* **87**, 243-257, doi:10.1016/j.neuro.2021.10.008 (2021).
114 Ashok, A. H. *et al.* The dopamine hypothesis of bipolar affective disorder: the state of the art and implications for treatment. *Mol Psychiatry* **22**, 666-679, doi:10.1038/mp.2017.16 (2017).
115 Geelhand de Merxem, R., Launay, S. & Hanak, C. Association Between Bipolar Disorder and Parkinson's Disease. *Psychiatr Danub* **35**, 66-71 (2023).
116 Chen, Y. *et al.* Non-Genetic Risk Factors for Parkinson's Disease: An Overview of 46 Systematic Reviews. *J Parkinsons Dis* **11**, 919-935, doi:10.3233/JPD-202521 (2021).
117 Kerner, B. *et al.* Polymorphisms in the GRIA1 gene region in psychotic bipolar disorder. *Am J Med Genet B Neuropsychiatr Genet* **150B**, 24-32, doi:10.1002/ajmg.b.30780 (2009).
118 Hoppmann, V., Wu, J. J., Soviknes, A. M., Helvik, J. V. & Becker, T. S. Expression of the eight AMPA receptor subunit genes in the developing central nervous system and sensory organs of zebrafish. *Dev Dyn* **237**, 788-799, doi:10.1002/dvdy.21447 (2008).
119 Saitoh, O. & Yoshihiro, K. Biochemical and electrophysiological analyses of RGS8 function. *Methods Enzymol* **390**, 129-148, doi:10.1016/S0076-6879(04)90009-2 (2004).
120 Rahman, N., Stewart, G. & Jones, G. A role for the atopy-associated gene PHF11 in T-cell activation and viability. *Immunol Cell Biol* **88**, 817-824, doi:10.1038/icb.2010.57 (2010).
121 Dominguez Cadena, L. C. *et al.* Rab6b localizes to the Golgi complex in murine macrophages and promotes tumor necrosis factor release in response to mycobacterial infection. *Immunol Cell Biol* **99**, 1067-1076, doi:10.1111/imcb.12503 (2021).
122 Wagnon, J. L. *et al.* CELF4 regulates translation and local abundance of a vast set of mRNAs, including genes associated with regulation of synaptic function. *PLoS Genet* **8**, e1003067, doi:10.1371/journal.pgen.1003067 (2012).
123 Scuderi, C. *et al.* Biallelic intragenic duplication in ADGRB3 (BAI3) gene associated with intellectual disability, cerebellar atrophy, and behavioral disorder. *Eur J Hum Genet* **27**, 594-602, doi:10.1038/s41431-018-0321-1 (2019).
124 Kone, A. S., Ait Ssi, S., Sahraoui, S. & Badou, A. BTN3A: A Promising Immune Checkpoint for Cancer Prognosis and Treatment. *Int J Mol Sci* **23**, doi:10.3390/ijms232113424 (2022).
125 Nakagawa, T. *et al.* Expression of the pacemaker channel HCN4 in excitatory interneurons in the dorsal horn of the murine spinal cord. *Mol Brain* **13**, 127, doi:10.1186/s13041-020-00666-6 (2020).
126 Gumy, L. F. *et al.* The kinesin-2 family member KIF3C regulates microtubule dynamics and is required for axon growth and regeneration. *J Neurosci* **33**, 11329-11345, doi:10.1523/JNEUROSCI.5221-12.2013 (2013).
127 Ageta-Ishihara, N. *et al.* Septin 3 regulates memory and L-LTP-dependent extension of endoplasmic reticulum into spines. *Cell Rep* **44**, 115352, doi:10.1016/j.celrep.2025.115352 (2025).
128 Ray, S. *et al.* Functional requirements for a Samd14-capping protein complex in stress erythropoiesis. *Elife* **11**, doi:10.7554/eLife.76497 (2022).

Abbreviations

PD	Parkinson's Disease
DA	Dopaminergic Neurons
SH-SY5Y	Human Neuroblastoma Cell Line
SN	Substantia Nigra
MPTP	1-Methyl-4-Phenyl-1,2,3,6-Tetrahydropyridine
qRT-PCR	Quantitative Reverse Transcription Polymerase Chain Reaction
PPI	Protein-Protein Interaction
GO	Gene Ontology
GEO	Gene Expression Omnibus
DEGs	Differentially Expressed Genes
cDEGs	Common Differentially Expressed Genes
iPSCs	Induced Pluripotent Stem Cells
GWAS	Genome-Wide Association Study
BTN3A2	Butyrophilin Subfamily 3 Member A2
GRIA1	Glutamate Ionotropic Receptor AMPA Type Subunit 1
PSMB8	Proteasome Subunit Beta Type-8
HCN4	Hyperpolarization-Activated Cyclic Nucleotide-Gated Potassium Channel 4
RGS8	Regulator of G Protein Signaling 8
CELF3	CUGBP Elav-Like Family Member 3
SEPTIN3	Septin 3
GPCR	G Protein-Coupled Receptor
PHF11	Plant Homeodomain Finger Protein 11
PARK2	Parkinsonism Associated Deglycase (Parkin)
LRRK2	Leucine-Rich Repeat Kinase 2
PINK1	PTEN-Induced Kinase 1
DJ-1	Protein Deglycase DJ-1
SNCA	Synuclein Alpha
GBA	Glucocerebrosidase
DisGeNET	Disease Gene Association Network
DAVID	Database for Annotation, Visualization, and Integrated Discovery
MCODE	Molecular Complex Detection
DMSO	Dimethyl Sulfoxide
IPTG	Isopropyl β-D-1-Thiogalactopyranoside
LB	Luria-Bertani Medium
NGM	Nematode Growth Medium
RNAi	RNA Interference
FC	Fold Change
L1	First Larval Stage

Figure Legends

Figure 1. Gene expression analysis of the three selected datasets. (A) Bar graph of up- and downregulated genes in PD vs healthy DA neurons from each dataset. (B) Volcano plots to demonstrate gene expression differences between PD and control groups in the datasets. The criteria for selection of differentially expressed genes was set $p \leq 0.05$ and $|\log_2 FC| \geq 0.5$. (C) In all three datasets, 21 genes were upregulated, and 19 genes were downregulated, as depicted in the Venn diagram. (D) Bar Graph showing the $\log_2$FC of upregulated genes in PD vs. Control DA neurons in respective datasets. (E) Bar Graph showing the $\log_2$FC of downregulated genes in PD vs. Control DA neurons in respective datasets.

Figure 2. The Protein-Protein Interaction network and modular analysis of cDEGs. (A) The 40 cDEGs were filtered into the PPI network complex using the GENEMANIA plugin in the Cytoscape software. The network nodes include proteins encoded by the cDEGs and genes other than cDEGs. The edges represent their functional associations. (B) The three most significant modules within the PPI network were identified using the MCODE plugin in the Cytoscape software. The black arrowhead denotes cDEGs. (C) GO and Reactome pathway enrichment analysis of the hub genes.

Figure 3. Hub Gene-Disease Interaction network created by Networkanalyst tool. Gene-Disease Interaction network of (A) PSMB8, (B) GRIA1, (C) HCN4, and (D) PHF11.

Figure 4. Expression profiles of hub genes in MPTP-treated SH-SY5Y cell model of PD versus untreated cells. Relative fold-change of (A) upregulated and (B) downregulated hub genes as validated by qPCR. mRNA for GAPDH was used for normalization. The data is represented as mean ± standard deviation. n = 3. * $p<0.005$, ** $p<0.01$; Unpaired t-test

Figure 5. *Rgs8* RNAi affects DA neuronal health in *C. elegans*. (A) Fluorescence images of DA neurons within the head region of BY250 (Control RNAi), BY250 (*rgs8* RNAi), and UA44 (Control RNAi). (B) Graph showing fluorescence intensities of DA neurons in the head region as quantified by ImageJ software. The data is represented as mean ± standard deviation. $n \geq 20$. ** $p<0.01$; **** $p<0.0001$; Unpaired t-test. (C) qRT-PCR data for *rgs8* mRNA in BY250 (Control RNAi), BY250 (*rgs8* RNAi) and UA44 (Control RNAi). mRNA for *actinb* was used for normalization. The data is represented as mean ± standard deviation. n=3. * $p<0.05$; **** $p<0.0001$; Unpaired t-test.

Table 1: GEO studies included in the analysis

S. No.	GSE	Experiment Type	No. of Samples	Mutation associated with PD	Sample Type
1	GSE90469	High-throughput sequencing	PD-3; Control-3	Familial (*LRRK2*)	human iPSC-derived neurons
2	GSE169755	High-throughput sequencing	PD-6; Control-6	Idiopathic	laser-captured dopaminergic neurons from postmortem human tissue
3	GSE181029	High-throughput sequencing	PD-9; Control-6	Familial (*PARK2*)	human iPSC-derived neurons

Table 2: Overview of samples used for GEO2R analysis in each dataset.

GSE	Sample Accession	Mutation associated
GSE90469	GSM3402505	G2019S *LRRK2*
	GSM3402506	G2019S *LRRK2*
	GSM3402507	G2019S *LRRK2*
	GSM3402502	Control
	GSM3402503	Control
	GSM3402504	Control
GSE169755	GSM5213623	Idiopathic
	GSM5213624	Idiopathic
	GSM5213627	Idiopathic
	GSM5213628	Idiopathic
	GSM5213633	Idiopathic
	GSM5213634	Idiopathic
	GSM5213625	Control
	GSM5213626	Control
	GSM5213629	Control
	GSM5213630	Control
	GSM5213631	Control
	GSM5213632	Control
GSE181029	GSM5482235	*PARK2*: 2 exon (del 202-203 AG), 1 intron (splicing mutation IVS1+1G/A)
	GSM5482236	*PARK2*: 2 exon (del 202-203 AG), 1 intron (splicing mutation IVS1+1G/A)

GSM5482237	*PARK2*: 2 exon (del 202-203 AG), 1 intron (splicing mutation IVS1+1G/A)
GSM5482238	*PARK2*: heterozygous deletion of 8 exon
GSM5482239	*PARK2*: heterozygous deletion of 8 exon
GSM5482240	*PARK2*: heterozygous deletion of 8 exon
GSM5482241	*PARK2*: heterozygous deletion of 2 exon
GSM5482242	*PARK2*: heterozygous deletion of 2 exon
GSM5482243	*PARK2*: heterozygous deletion of 2 exon
GSM5482229	Control
GSM5482230	Control
GSM5482231	Control
GSM5482232	Control
GSM5482233	Control
GSM5482234	Control

Table 3: GO and Reactome Pathway Analysis of Hub Genes by DAVID.

Category	Term	%	PValue	Genes	Fold Enrichment
GOTERM_BP_DIRECT	GO:0019722~calcium-mediated signaling	16.67	0.06	GRIA1, SAMD14	29.92
GOTERM_BP_DIRECT	GO:0031175~neuron projection development	16.67	0.06	SAMD14, RAB6B	27.58
GOTERM_CC_DIRECT	GO:0030425~dendrite	33.33	0.00	HCN4, GRIA1, SAMD14, RGS8	14.81
GOTERM_CC_DIRECT	GO:0098793~presynapse	25	0.01	GRIA1, SEPTIN3, RAB6B	24.03
GOTERM_CC_DIRECT	GO:0032809~neuronal cell body membrane	16.67	0.02	GRIA1, RGS8	114.81
GOTERM_MF_DIRECT	GO:0031489~myosin V binding	16.67	0.01	GRIA1, RAB6B	188.31
GOTERM_MF_DIRECT	GO:0003924~GTPase activity	25	0.02	SEPTIN3, RGS8, RAB6B	13.72
REACTOME_PATHWAY	R-HSA-199991~Membrane Trafficking	25	0.04	GRIA1, KIF3C, RAB6B	7.53
REACTOME_PATHWAY	R-HSA-5653656~Vesicle-mediated transport	25	0.05	GRIA1, KIF3C, RAB6B	7.09

Table 4: Potential Role of Hub Genes in DA neurodegeneration

S.no.	Hub Gene	Protein Encoded	Expression in GSE90469, GSE169755, and GSE181029 (PD vs. control)	Reported Cellular Function	Reported PD-association	Potential Role in DA-neurodegeneration
1	*PSMB8*	Proteasome subunit beta type-8	Upregulated	Part of 20S proteasome complex [105]	Yes [105]	May affect the clearance of misfolded or aggregated proteins
2	*GRIA1*	Glutamate receptor 1	Downregulated	Subunit of the AMPA-type glutamate receptor [118]	Yes [106]	May disrupt synaptic signaling and exacerbate excitotoxic stress
3	*RGS8*	Regulator of G-protein signaling 8	Downregulated	Regulate G protein-coupled receptor [119]	Yes [107]	May exacerbate immune-mediated neurotoxicity
4	*PHF11*	Plant Homeodomain Finger 11	Upregulated	Regulate transcription and inflammatory signaling pathways [120]	No	May promote a pro-inflammatory environment and alter stress response pathways
5	*RAB6B*	Ras-related protein Rab-6B	Downregulated	Regulate vesicle trafficking and transport within the Golgi complex [121]	No	May impair the clearance of aggregated proteins
6	*CELF3*	CUGBP Elav-Like Family Member 3	Downregulated	Regulate RNA processing, including cotranscriptional and post-transcriptional events [122]	No	May impair gene regulation
7	*ADGRB3*	Adhesion G Protein-Coupled Receptor B3	Downregulated	Regulate synapse formation and maintenance [123]	No	May impair synaptic function
8	*BTN3A2*	Butyrophilin Subfamily 3 Member A2	Upregulated	Regulate adaptive immune response and immune checkpoint regulation [124]	No	May mediate immune-driven neuronal injury
9	*HCN4*	Hyperpolarization Activated Cyclic Nucleotide Gated Potassium Channel 4	Downregulated	Regulate neuronal excitability [125]	No	May disrupt DA neuronal pacemaking and calcium homeostasis.

10	*KIF3C*	Kinesin family member 3C	Downregulated	Regulate neuronal development and axon growth and regeneration [126]	No	May exacerbate axonal pathology
11	*SEPTIN3*	Septin 3	Downregulated	Regulate memory and long-term potentiation [127]	No	May disrupt synaptic homeostasis
12	*SAMD14*	Sterile Alpha Motif Domain Containing 14	Downregulated	Regulate stress response pathways [128]	No	May compromise neuronal stress responses

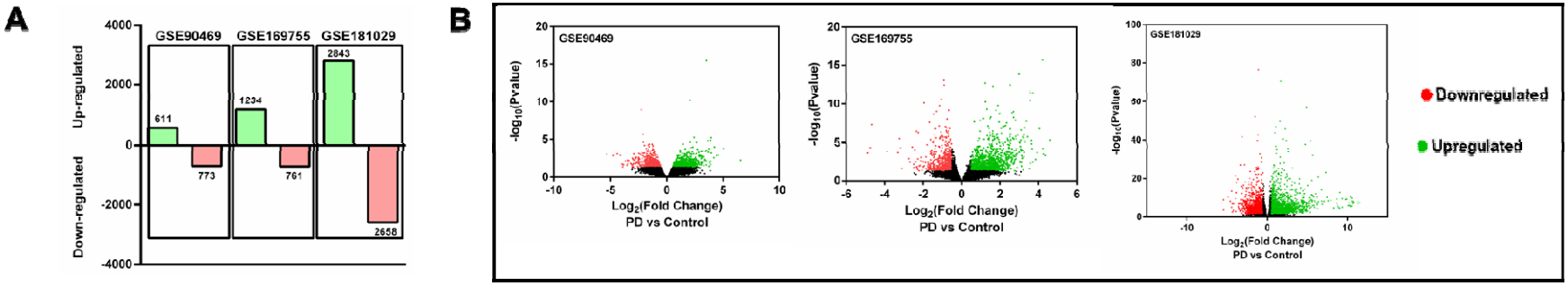

GSE90469- Familial (*LRRK2*) iPSC differentiated into dopaminergic neurons
GSE169755- Idiopathic laser-captured dopaminergic neurons from post-mortem human tissue
GSE181029- Familial (PARK2) iPSC differentiated into dopaminergic neurons

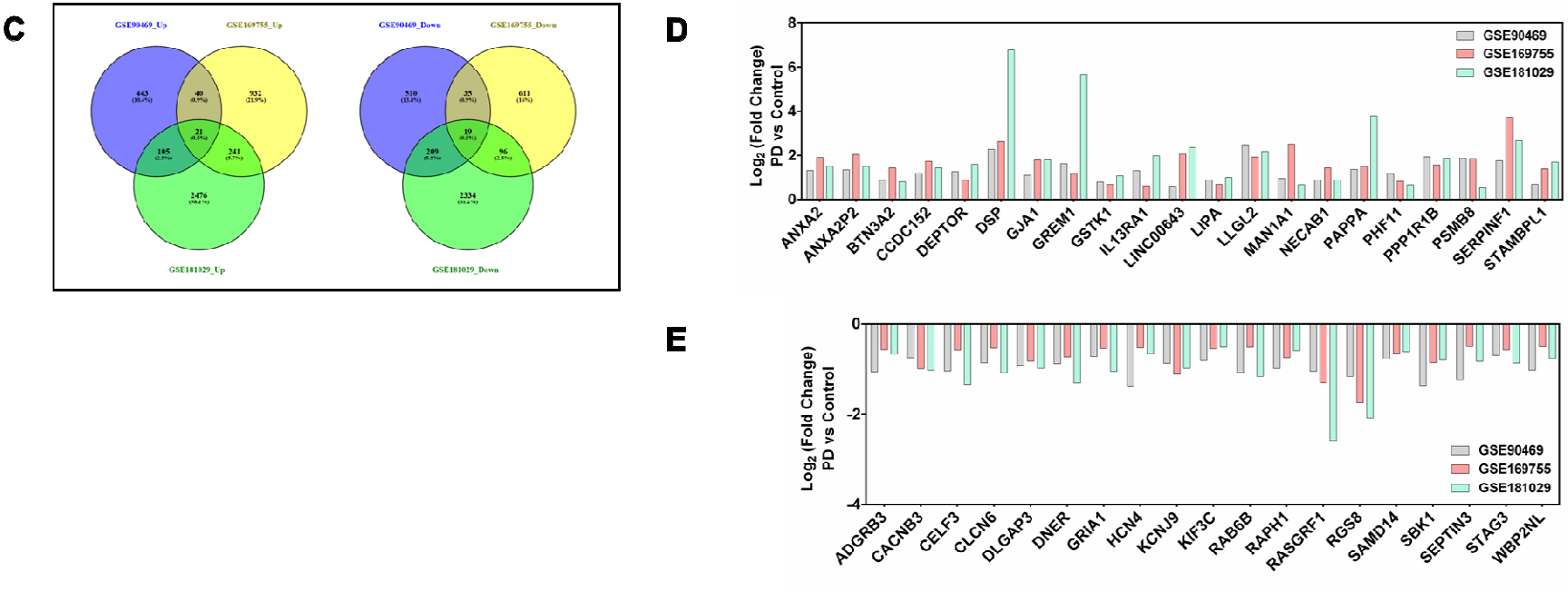

Figure 1

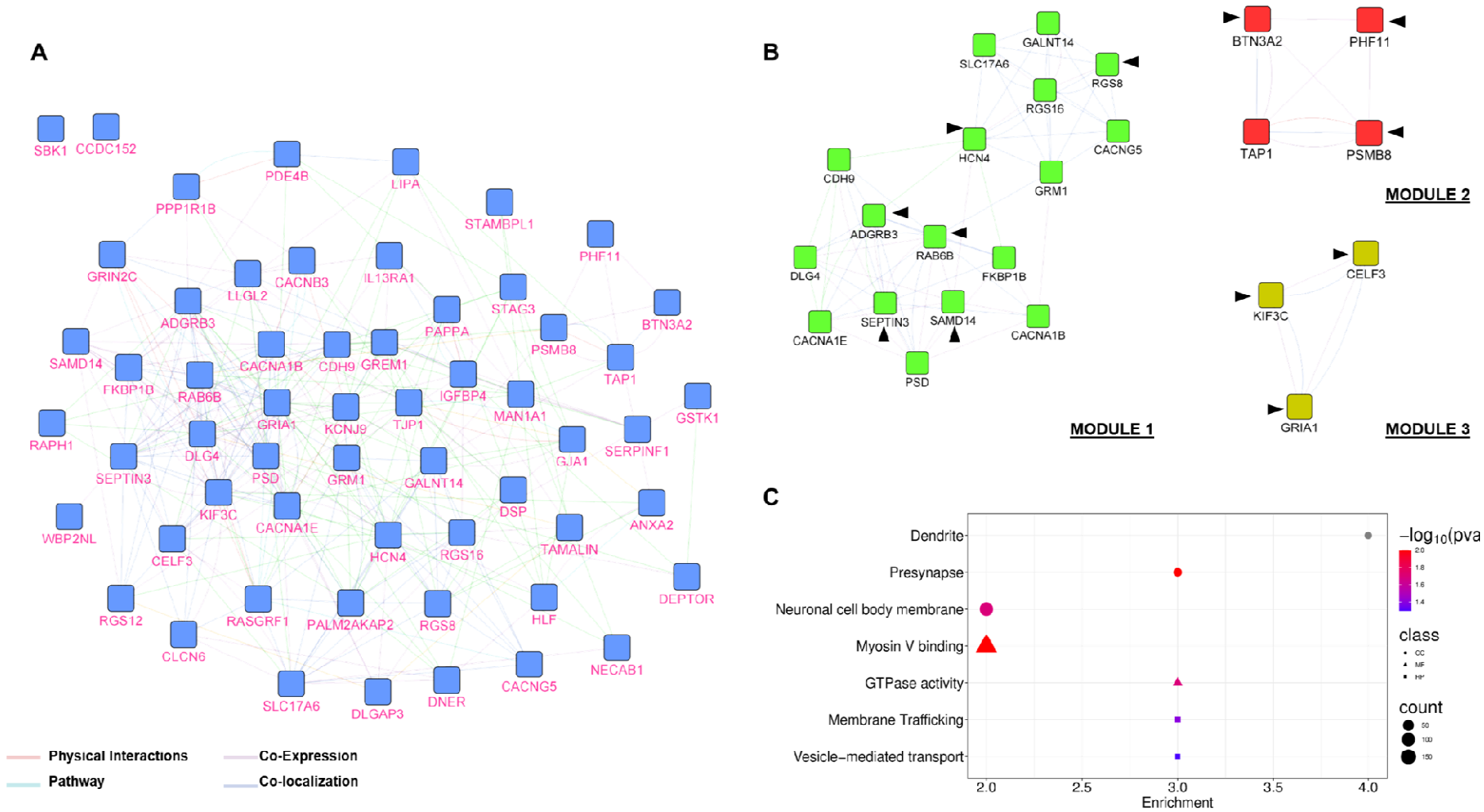
A
SBK1
CCDC152
PDE4B
LIPA
PPP1R1B
STAMBPL1
PHF11
GRIN2C
LLGL2
CACNB3
IL13RA1
STAG3
ADGRB3
PAPPA
BTN3A2
PSMB8
SAMD14
CACNA1B
CDH9
GREM1
TAP1
FKBP1B
RAB6B
IGFBP4
MAN1A1
GSTK1
GRIA1
KCNJ9
TJP1
RAPH1
DLG4
GJA1
SERPINF1
SEPTIN3
PSD
GRM1
GALNT14
KIF3C
DSP
CACNA1E
ANXA2
WBP2NL
HCN4
RGS16
TAMALIN
CELF3
DEPTOR
RGS12
RASGRF1
PALM2AKAP2
RGS8
HLF
CLCN6
NECAB1
CACNG5
SLC17A6
DNER
DLGAP3
Physical Interactions
Co-Expression
Pathway
Co-localization
B
GALNT14
SLC17A6
RGS8
RGS16
HCN4
CACNG5
CDH9
GRM1
ADGRB3
RAB6B
DLG4
FKBP1B
SEPTIN3
SAMD14
CACNA1E
CACNA1B
PSD
MODULE 1
BTN3A2
PHF11
TAP1
PSMB8
MODULE 2
CELF3
KIF3C
GRIA1
MODULE 3
C
Dendrite
Presynapse
Neuronal cell body membrane
Myosin V binding
GTPase activity
Membrane Trafficking
Vesicle−mediated transport
2.0
2.5
3.0
3.5
4.0
Enrichment
−log10(pva
class
count

Figure 2

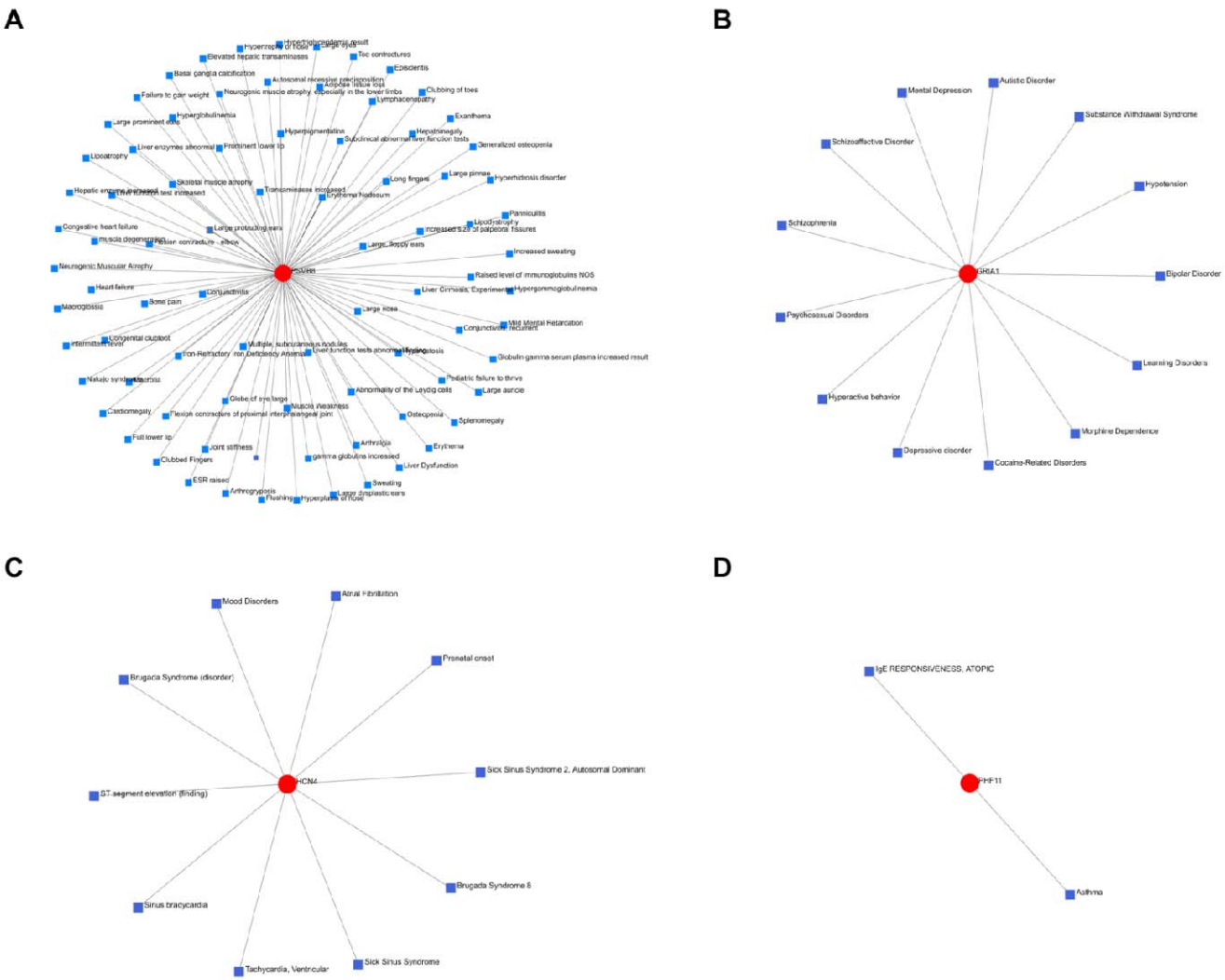
A
B
C
D
Mental Depression
Autistic Disorder
Substance Withdrawal Syndrome
Schizoaffective Disorder
Hypotension
Schizophrenia
GRIA1
Bipolar Disorder
Psychosexual Disorders
Learning Disorders
Hyperactive behavior
Morphine Dependence
Depressive disorder
Cocaine-Related Disorders
Mood Disorders
Atrial Fibrillation
Prenatal onset
Brugada Syndrome (disorder)
Sick Sinus Syndrome 2, Autosomal Dominant
HCN4
ST segment elevation (finding)
Brugada Syndrome 8
Sinus bradycardia
Tachycardia, Ventricular
Sick Sinus Syndrome
IgE RESPONSIVENESS, ATOPIC
FHF11
Asthma

Figure 3

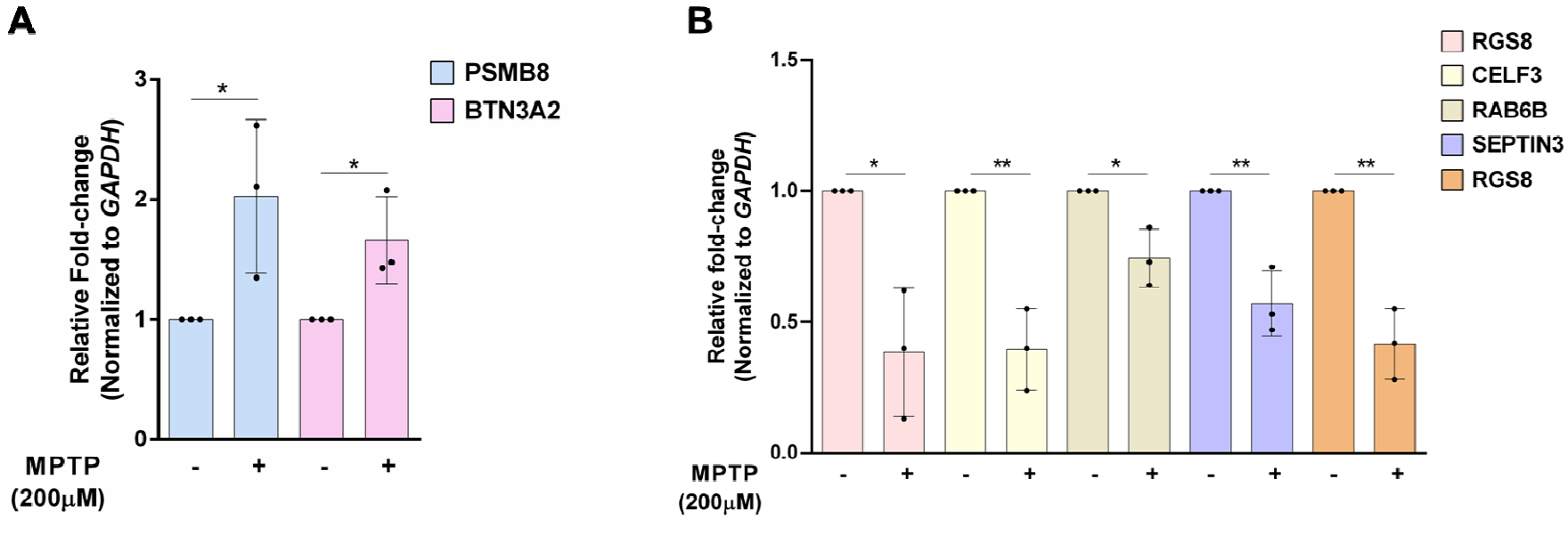
A
PSMB8
BTN3A2
Relative Fold-change
(Normalized to GAPDH)
3
2
1
0
*
*
MPTP
(200μM)
-
+
-
+
B
RGS8
CELF3
RAB6B
SEPTIN3
RGS8
Relative fold-change
(Normalized to GAPDH)
1.5
1.0
0.5
0.0
*
**
*
**
**
MPTP
(200μM)
-
+
-
+
-
+
-
+
-
+

Figure 4

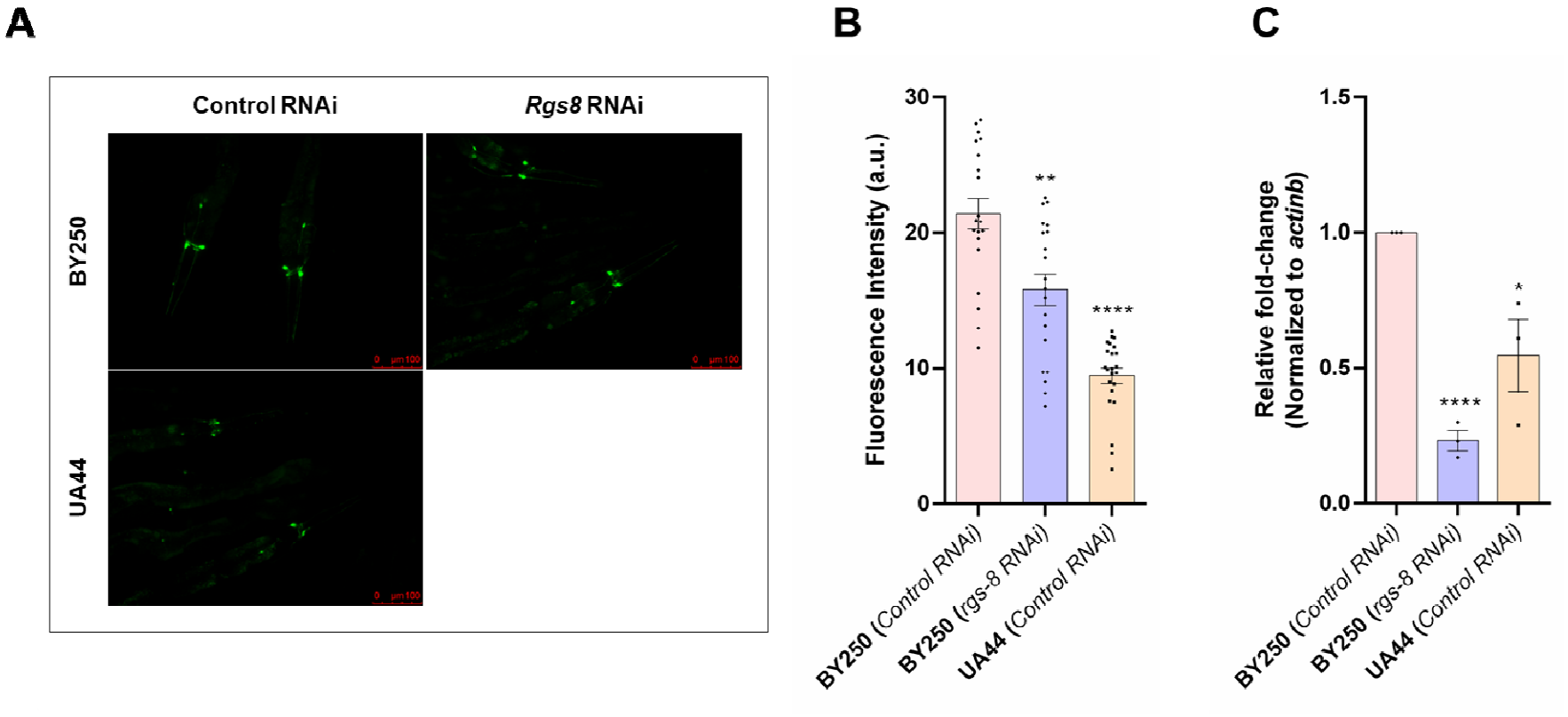
A
Control RNAi
Rgs8 RNAi
BY250
UA44
B
Fluorescence Intensity (a.u.)
30
20
10
0
**
****
BY250 (Control RNAi)
BY250 (rgs-8 RNAi)
UA44 (Control RNAi)
C
Relative fold-change
(Normalized to actinb)
1.5
1.0
0.5
0.0
****
*
BY250 (Control RNAi)
BY250 (rgs-8 RNAi)
UA44 (Control RNAi)

Figure 5

Supplementary Table 1: Sequence of Primers used for qRT-PCR

Target	Species	Primer	Sequence
BTN3A2	*H. sapiens*	Forward	GTCCAGTGAGATAGAAAGTGAGC
		Reverse	TGGTATCGGACGAAGACTCCTC
PSMB8	*H. sapiens*	Forward	CCTTACCTGCTTGGCACCATGT
		Reverse	TTGGAGGCTGCCGACACTGAAA
RGS8	*H. sapiens*	Forward	GTGAGGAGTTCAAGAAGACCAGG
		Reverse	CAGGTTCTTCCTCGTGGCTTCT
CELF3	*H. sapiens*	Forward	GGTCGGATCTTTGAGCTGACTG
		Reverse	GGAAGCGTCTTCTGTTCGTGCA
RAB6B	*H. sapiens*	Forward	CAACAAGACGGACCTGGCTGAT
		Reverse	CGTTGTAGCCAGTCTTCGCACT
SEPTIN3	*H. sapiens*	Forward	AGCGGCTCAATGACAATGGAGG
		Reverse	GAGGAATGGAGTGAGAAGCAGC
HCN4	*H. sapiens*	Forward	TCTACTCGCTGAGCGTGGACAA
		Reverse	GAGTTGAGGTCGTGCTGGACTT
GAPDH	*H. sapiens*	Forward	GTCTCCTCTGACTTCAACAGCG
		Reverse	ACCACCCTGTTGCTGTAGCCAA
Rgs8	*C. elegans*	Forward	GAATGTTTGACGGAAAGGAG
		Reverse	CAGAGATTGGAACAAGAACAC
Act-1	*C. elegans*	Forward	GCTGGACGTGATCTTACTGATTACC
		Reverse	GTAGCAGAGCTTCTCCTTGATGTC